Leptin Signaling Suppression in Macrophages Improves Immunometabolic Outcomes in Obesity

Lauar de Brito Monteiro,[1] Juliana Silveira Prodonoff,[1] Cristhiane Favero de Aguiar,[1] Felipe Correa-da-Silva,[1] Angela Castoldi,[2] Nikki van Teijlingen Bakker,[3] Gustavo Gastão Davanzo,[1] Bianca Castelucci,[1] Jéssica Aparecida da Silva Pereira,[1,4] Jonathan Curtis,[3,5] Jörg Büscher,[3] Larissa Menezes dos Reis,[1] Gisele Castro,[1] Guilherme Ribeiro,[1] João Victor Virgílio-da-Silva,[1] Douglas Adamoski,[6] Sandra Martha Gomes Dias,[6] Silvio Roberto Consonni,[7] Jose Donato Jr.,[8] Edward J. Pearce,[3,5] Niels Olsen Saraiva Câmara,[4] and Pedro M. Moraes-Vieira[1,9,10]

Diabetes 2022;71:1546–1561 | https://doi.org/10.2337/db21-0842

Obesity is a major concern for global health care systems. Systemic low-grade inflammation in obesity is a major risk factor for insulin resistance. Leptin is an adipokine secreted by the adipose tissue that functions by controlling food intake, leading to satiety. Leptin levels are increased in obesity. Here, we show that leptin enhances the effects of LPS in macrophages, intensifying the production of cytokines, glycolytic rates, and morphological and functional changes in the mitochondria through an mTORC2-dependent, mTORC1-independent mechanism. Leptin also boosts the effects of IL-4 in macrophages, leading to increased oxygen consumption, expression of macrophage markers associated with a tissue repair phenotype, and wound healing. In vivo, hyperleptinemia caused by diet-induced obesity increases the inflammatory response by macrophages. Deletion of leptin receptor and subsequently of leptin signaling in myeloid cells (ObR$^{-/-}$) is sufficient to improve insulin resistance in obese mice and decrease systemic inflammation. Our results indicate that leptin acts as a systemic nutritional checkpoint to regulate macrophage fitness and contributes to obesity-induced inflammation and insulin resistance. Thus, specific interventions aimed at downstream modulators of leptin signaling may represent new therapeutic targets to treat obesity-induced systemic inflammation.

Leptin is an adipokine produced by the adipose tissue (AT) and regulates food intake (1,2). Leptin is known to have proinflammatory effects (3). Leptin activates the STAT3 pathway as well as the phosphatidylinositol 3-kinase (PI3K)/mammalian target of rapamycin (mTOR) pathway (3–5). mTOR is an intracellular kinase that integrates nutrients signaling from growth factors present in the microenvironment (leptin, insulin, IL-2) to define the global metabolic rate and determine cellular growth, proliferation, and response (4,6). Animals deficient in leptin or leptin receptor present several metabolic and immunologic alterations.

[1]Laboratory of Immunometabolism, Department of Genetics, Evolution, Microbiology and Immunology, University of Campinas, Campinas, Brazil
[2]Laboratory Keizo Asami, Immunopathology Laboratory, Federal University of Pernambuco, Pernambuco, Brazil
[3]Department of Immunometabolism, Max Planck Institute of Epigenetics and Immunobiology, Freiburg im Breisgau, Germany
[4]Department of Immunology, Institute of Biomedical Sciences IV, University of São Paulo, São Paulo, Brazil
[5]Bloomberg Kimmel Institute and Department of Oncology, Johns Hopkins University School of Medicine, Baltimore, MD
[6]Brazilian Biosciences National Laboratory (LNBio), Brazilian Center for Research in Energy and Materials (CNPEM), Campinas, Brazil
[7]Department of Biochemistry and Tissue Biology, Institute of Biology, University of Campinas, Campinas, Brazil
[8]Department of Physiology and Biophysics, Institute of Biomedical Sciences, University of São Paulo, São Paulo, Brazil
[9]Experimental Medicine Research Cluster, University of Campinas, São Paulo, Brazil
[10]Obesity and Comorbidities Research Center, University of Campinas, São Paulo, Brazil

Corresponding author: Pedro M. Moraes-Vieira, pmvieira@unicamp.br

Received 17 September 2021 and accepted 13 March 2022

This article contains supplementary material online at https://doi.org/10.2337/figshare.19411349.

Circulating levels of leptin are increased in obesity due to AT expansion and central leptin resistance (7,8). This is also associated with insulin resistance, which is the major risk factor for type 2 diabetes (9–11). AT inflammation is closely related to insulin resistance, and AT macrophages (ATMs) are key mediators of AT inflammation (8,12). ATMs contribute to systemic low-grade inflammation observed in obesity by releasing proinflammatory cytokines, such as TNF-α, IL-6, IL-12, and IL-1β, which impair insulin signaling in adipocytes (9,10,12, 13). ATMs are extremely plastic cells and can present a large spectrum of activation phenotypes in a context-dependent way. Two extreme macrophage activation phenotypes are the proinflammatory (M1) and tissue repair/anti-inflammatory (M2) phenotypes (8,14). In both activation states, macrophages exhibit increased glucose utilization to meet metabolic needs to fulfill their function (15,16). On inflammatory signaling, macrophages undergo intense metabolic reprogramming, favoring a metabolic shift toward glycolysis and reduced oxidative respiration (17,18). Tissue-derived factors can modulate macrophage immunometabolic profile and function. For example, chronic exposure to insulin promotes a unique macrophage phenotype—with M2-like features and increased glycolysis (19,20). Also, macrophages treated with leptin accumulate lipid droplets, which is a hallmark of macrophage commitment to an inflammatory state (21,22). Thus, tissue-derived factors, such as leptin, may modulate the immunometabolic profile of macrophages, contributing to obesity-induced systemic inflammation and insulin resistance.

Understanding how hyperleptinemia modulates macrophage metabolism and function is of paramount importance to understanding the mechanisms associated with obesity-induced disorders, such as type 2 diabetes. Here, we explored the importance of leptin effects in macrophages and the consequences for the metabolic and inflammatory outcomes of obesity. We show that leptin acts as a checkpoint for macrophage activation. It exacerbates the activation of macrophages triggered by LPS and IL-4 with metabolic and functional consequences. Moreover, peritoneal macrophages (pMacs) from obese and hyperleptinemic mice have elevated expression of proinflammatory cytokines and leptin receptor (LepR or ObR), as well as increased mTOR activity, which are not triggered in ATMs. Loss of leptin signaling in myeloid cells improves systemic glucose homeostasis in hyperleptinemic obese mice and reduces systemic low-grade inflammation. These findings support the model where tissue-derived cues modulate immune cells function and metabolism, affecting systemic inflammation in obesity, which brings focus to novel potential therapeutic targets downstream of leptin signaling.

RESEARCH DESIGN AND METHODS

Animal Use

Male C57BL6, LysMcre, *ob/ob*, and *db/db* mice at 6–12 weeks of age were obtained from the Multidisciplinary Center for Biological Investigation on Laboratory Animal Science (CEMIB). ObRLoxp (B6.129P2-*Lepr*^{tm1Rck}/J), RaptorLoxp (B6.Cg-*Rptor*$^{tm2.1Lex}$/J, Rap^{loxP}), and RictorLoxp (*Rictor*$^{tm1.1Klg}$/SjmJ) mice were purchased from The Jackson Laboratory. The ObR-reporter tdTomato animals were obtained from the Institute of Biomedical Sciences, University of São Paulo. The use of animals was approved by the Research Ethics Committee (Comissão de Ética na Utilização Animal: 4493-1/2017). High-fat diet (HFD) TD93075 was acquired from Harlan Teklad. Blood glucose was determined with a One Touch Basic glucometer (LifeScan).

Insulin Tolerance Test and Glucose Tolerance Test

These tests were performed after either 5 h (insulin tolerance test [ITT]) or 12–14 h (glucose tolerance test [GTT]) of fasting as previously described (23).

Macrophage Isolation and Primary Cell Culture

Perigonadal AT (pgAT) was removed, cut into small pieces in RPMI medium + 2% FBS, and digested for ∼40 min with collagenase type II (Sigma-Aldrich). Cell suspensions were then filtered through a sieve and centrifugated. The peritoneal lavage was collected with use of 5 mL PBS + 2% FBS, and the cells were separated by centrifugation for further staining for flow cytometry. Bone marrow–derived macrophages were obtained as previously described (24).

Flow Cytometry

Macrophages were resuspended in PBS supplemented with 2% FBS. Surface markers were stained with monoclonal antibody for multicolor flow cytometry (Table 1) diluted in PBS + 2% FBS (1:200) for 30 min. Mitochondrial staining was performed as previously described (25). For intracellular staining, cells were stimulated with phorbol 12-myristate 13-acetate (50 ng/mL) and ionomycin (1 nmol/L) for 4 h. Brefeldin was added to the culture during the last 3 h. Cells were then permeabilized and fixed with CytoFix/CytoPerm (BD Biosciences). Cells were washed with BD Perm/Wash Buffer (BD Biosciences) to maintain the cells permeabilized. Cytokines and phosphorylated proteins were stained with monoclonal antibody (Table 1) diluted in BD Perm/Wash Buffer (1:200) for 40 min. Stained cells were washed with PBS and acquired with a BD LSRFortessa or BD FACSymphony flow cytometer (BD Biosciences) and analyzed with FlowJo software (Tree Star).

Cytokine Production

Cytokine release in supernatant after leptin (100 ng/mL) and/or LPS (100 ng/mL) was measured with ELISA using capture and detection antibodies against TNF-α, IL-6, and IL-12 (eBioscience) according to the manufacturer's protocols.

Metabolite Quantification Using Bioanalyzer

Macrophage supernatant was analyzed on Cedex Bio Analyzer (Roche) with use of Glutamine V2 Bio, Lactate Bio,

Table 1—Antibodies panel for flow cytometry

Marker	Fluorochrome	Clone
F4/80	PECy7	BM8 (BioLegend)
F4/80	BV421	BM8 (BioLegend)
F4/80	BV650	BM8 (BioLegend)
CD11b	APCCy7	M1/70 (BioLegend)
CD11c	BV421	N418 (BD Biosciences)
CD45	PercpCy5.5	30-F11 (BioLegend)
CD45	V500	30-F11 (BD Biosciences)
CD206	FITC	C068C2 (BioLegend)
CD206	PECY7	C068C2 (BioLegend)
TIM4	BV711	21H12 (BD Biosciences)
TNF-α	PECy7	MP6-XT22 (BioLegend)
IL-10	PE	JES5-16E3 (BioLegend)
IL-10	BV605	JES5-16E3 (BD Biosciences)
IL-1β	PE	NJTEN3 (Invitrogen)
IL-12	APC	C15.6 (BioLegend)
IL-6	APC	MP5-20F3 (BioLegend)
p-S6	Pacific Blue	D57.2.2E (BioLegend)
p-AKT^{Ser473}	PE	D9E (BioLegend)
p-STAT3	AF647	D3A7 (BioLegend)
Live/dead	V500 (Zombie Aqua)	Cat no. 423101 (BioLegend)
Live/dead	Near-IR	Cat no. L10119 (Invitrogen)
Live/dead	FITC (Zombie Green)	Cat no. 423111 (BioLegend)
MitoTracker Green	—	Cat no. M7514 (Invitrogen)
MitoTracker Red	—	Cat no. M7512 (Invitrogen)

APC, allophycocyanin; PE, phycoerythrin.

and Glucose Bio test kits according to the manufacturer's instructions.

Real-time PCR

Total RNA was isolated and purified with RNeasy Mini Kit (QIAGEN). cDNA was synthesized with SuperScript III First-Strand Synthesis System (Invitrogen). Real-time PCR was applied with TaqMan probes (Applied Biosystems). Expression levels of each gene (Table 2) were normalized to housekeeping gene HPRT.

Seahorse Assay

For real-time analysis of ECAR (extracellular acidification rate) and OCR (oxygen consumption rate), macrophages were analyzed with an XFe24 or XFe96 Extracellular Flux Analyzer (Seahorse Bioscience) according to the manufacturer's instructions. Three or more consecutive measurements were obtained under baseline conditions and after the sequential addition of specific inhibitors/activators from the metabolic tests. For the mitochondrial stress test, we added 1 μmol/L oligomycin, 1.5 μmol/L FCCP (fluorocarbonyl cyanide phenylhydrazone), and 100 nmol/L rotenone + 1 μmol/L antimycin A (all Sigma-Aldrich reagents). For the glycolytic stress test, we added glucose (25 mmol/L), oligomycin (2 μmol/L), and 2-deoxyglucose (2-DG) (50 mmol/L).

Metabolite Extraction and Data Analysis

For carbon-tracing experiments, macrophages were stimulated for 1 h in the presence of ^{13}C glucose and then treated with leptin (100 ng/mL) and LPS (100 ng/mL) for 5 h. Metabolites from cultured cells were extracted through washing of the cell layer with ice-cold (4°C) 0.9% NaCl solution and addition of 500 μL extraction solution (80:20 methanol:Milli-Q water [stored at −80°C] with 1 μg/mL norvaline and 1 μg/mL adipic acid) to cells. Macrophages were then scraped and incubated 2–5 min on ice, and the extraction mix was transferred to Eppendorf tubes. We centrifuged the samples for 15 min, 10,000 relative centrifugal force, and transferred the supernatant to a new Eppendorf tube. Dried metabolite extracts were resuspended in pyridine and derivatized with 20 mg/mL methoxyamine (sc-263468; Santa Cruz Biotechnology) for 60 min at 37°C and subsequently with *N*-(*tert*-Butyldimethylsilyl)-N-methyltrifluoroacetamide, with 1% *tert*-Butyldimethylchlorosilane (375934; Sigma-Aldrich) for 60 min

Table 2—Oligonucleotide primer sequences for qPCR

Gene	Sequence
Il1b	Forward 5′-TACGAATCTCCGACCACCACTACAG-3′, reverse 5′-TGGAGGTGGAGAGCTTTCAGTTCATATG-3′
Il6	Forward 5′-TCCTCTCTGCAAGAGACTTCC-3′, reverse 5′-TTGTGAAGTAGGGAAGGCCG-3′
Il12	Forward 5′-ATGACCCTGTGCCTTGGTAG-3′, reverse 5′-CTGAAGTGCTGCGTTGATGG-3′
Il10	Forward 5′-GGCGCTGTCATCGATTTCTC-3′, reverse 5′-ATGGCCTTGTAGACACCTTGG-3′
Tnfa	Forward 5′-GATCGGTCCCCAAAGGGATG-3′, reverse 5′-GGTGGTTTGTGAGTGTGAGG-3′
Arg1	Forward 5′-ACAGGTAGGGAGAGTCTGAGG-3′, reverse 5′-GAGTTCCGAAGCAAGCCAAG-3′
Fizz1	Forward 5′-TAC TTG CAA CTG CCT GTG CTT ACT-3′, reverse 5′-TAT CAA AGC TGG GTT CTC CAC CTC-3′
Ym1	Forward 5′-TCT CTA CTC CTC AGA ACC GTC AGA-3′, reverse 5′-GAT GTT TGT CCT TAG GAG GGC TTC-3′
Mgl1/2	Forward 5′-TGAGAAAGGCTTTAAGAACTGGG-3′, reverse 5′-GACCACCTGTAGTGATGTGGG-3′
Mrc1	Forward 5′-GTCAGAACAGACTGCGTGGA-3′, reverse 5′-AGGGATCGCCTGTTTTCCAG-3′
Abca1	Forward 5′-AACAGTTTGTGGCCCTTTTG-3′, reverse 5′-AGTTCCAGGCTGGGGTACTT-3′
Cd36	Forward 5′-ATGGGCTGTGATCGGAATG-3′, reverse 5′-GTCTTCCCAATAAGCAGTGCTCC-3′
Plin2	Forward 5′-GACCTTGTGTCCTCGCTTAT-3′, reverse 5′-CAACCGCATTTGTGGCTC-3′
Stat3	Forward 5′-GGGTTGGTTGTTAGACAAGTGC-3′, reverse 5′-AGCAAGGTTGAAAGTGCAGAG-3′
LepR/ObR	Forward 5′-TCTGGAGCCTGAACCCATTTC-3′, reverse 5′-CTGCTGGGACCATCTCATCT-3′
18s (endogenous)	Forward 5′-CTCAACACGGGAAACCTCAC-3′, reverse 5′-CGCTCCACCAACTAAGAACG-3′

at 80°C. Isotopomer distributions were measured with a DB-5MS GC Column in a 7890 GC system (Agilent Technologies) combined with a 5977 MS system (Agilent Technologies). Data processing, including correction for natural isotope abundance, was performed as previously described (26,27).

Electron Microscopy

Electron microscopy was carried out at the Electron Microscopy Laboratory of the Institute of Biology at the University of Campinas. A cell monolayer grown on a glass coverslip was fixed with 2.5% glutaraldehyde in 0.1 mol/L sodium cacodylate and 3 mmol/L $CaCl_2$ buffer and incubated for 1 h on ice. After fixation, the samples were washed in 0.1 mol/L sodium cacodylate and 3 mmol/L $CaCl_2$ buffer and fixed with 2% osmium tetroxide in 0.1 mol/L sodium cacodylate and 3 mmol/L $CaCl_2$ buffer for 30 min and kept in acetate. Next, 2% uranyl was added and kept in the freezer overnight. The cells were dehydrated in ethanol on ice. The dehydrated cells were infiltrated in epon resin and placed in an oven at 60°C for polymerization for 72 h. Ultrathin cell slides were cut with a Leica Ultracut microtome, stained with 2% uranyl acetate and Reynolds citrate solution, and examined on a Leo 906 Transmission Electron Microscope (ZEISS) at an acceleration voltage of 60 kV.

Western Blotting

We incubated 50 μg protein that was extracted in radioimmunoprecipitation assay (RIPA) buffer (Sigma-Aldrich) and resuspended in NuPAGE LDS Sample Buffer 4X (Thermo Fisher Scientific). The samples were then heated at 95°C for 5 min. The protein concentrate was submitted to electrophoresis gel in polyacrilamide gel 8% under 120 V tension and 30 mA. After the electrophoresis migration, we performed immunoblotting by transferring the proteins into a nitrocellulose membrane Hybond ECL, Amersham Pharmacia Biotech (Uppsala, Sweden). The membrane was blocked with 5% albumin solution in Tris-buffered saline with Tween (Tris-HCl 200 mmol/L, NaCl 500 mmol/L, Tween20, pH 7.5) for 1 h before the overnight incubation at 4°C with specific primary antibody (Table 3). The secondary antibody was incubated for 1 h at room temperature, and we used SuperSignal West Pico PLUS Chemiluminescent Substrate (Thermo Fisher Scientific) to obtain the images according to the manufacturer's instructions.

Table 3—Primary antibodies used for Western blot

Target	Clone	Supplier
4E-BP1	53H11	Cell Signaling Technology
AKT (pan)	11E7	Cell Signaling Technology
Phospho-4E-BP1 (Thr37/46)	236B4	Cell Signaling Technology
p-AKT^{Ser473}	D9E	Cell Signaling Technology
OXPHOS (total)	Cat no. MS604/ab11041	Abcam

STAT3 shRNA

pLKO.1 lentiviral vector (Addgene plasmid no. 8453) was used to clone shRNAs targeting the genes of interest within the AgeI/EcoRI sites at the 3-end of the human U6 promoter. The targeted sequences were as follows: GFP 5′CAAGCTGACCCTGAAGTTCAT-3′, STAT3 5′-CGACTTTGATTTCAACTACAA-3′. Bone marrow–derived macrophages (BMDM) were transduced with lentiviral particles (multiplicity of infection 1) from the pLKO shGFP or pLKO shSTAT3 on the fourth day of differentiation in the presence of L929. On the fifth day, the cells received the selection antibiotic and were maintained with 1 μg/mL puromycin for another 5 days. Then, the cells were treated with 100 ng/mL leptin and/or 100 ng/mL LPS (6 h) or 20 ng/mL IL-4 (24 h) for gene expression assays. The knockdown was quantified with quantitative PCR (qPCR) with target primers for STAT3.

Wound Healing Assay

A total of 4,600 cells/mm^2 of BMDM were seeded and differentiated with L929. On the seventh day, cells were treated with 100 ng/mL leptin for 30 min. Next, wounds were created with 200 μL pipette tips and the wells were washed once with PBS. The cells were treated with 20 ng/mL IL4 in RPMI medium supplemented with 10% FBS and immediately imaged for 16 h with use of Operetta (PerkinElmer Life Sciences) in bright-field mode every hour at 37°C in a 5% CO_2 atmosphere. The images were processed with Fiji-ImageJ using a macro based on previous work (28).

Data Analysis

The data were analyzed with Student *t* test or one-way ANOVA, followed by the Tukey test or two-way ANOVA followed by the Holm-Sidak method to determine the significance of the individual differences. Data were analyzed with the statistical software SigmaStat 3.1 (Systat Software, Point Richmond, CA). Only male mice were used; thus, sex was not considered as a factor in the statistical analysis of the data.

Data and Resource Availability

Further information, reagents, and all other supporting data in this study are available on request from corresponding author Pedro M. Moraes-Vieira.

RESULTS

Leptin Potentiates LPS-Induced Metabolic Reprogramming in Macrophages

We found that leptin treatment prior to LPS activation led to increased mRNA expression and secretion of the proinflammatory cytokines TNF-α, IL-12, and IL-6 (Fig. 1*A* and *B*). Leptin treatment of LPS-activated macrophages from wild-type (WT) and leptin-deficient (*ob/ob*) mice led to enhanced LPS-induced cytokine production in macrophages (Supplementary Fig. 1*B* and *C*). Leptin had no additive effect of LPS-induced changes in pMacs and BMDM from leptin receptor–deficient (*db/db*) mice (Supplementary Fig. 1*A*–*C*). We observed that, in *ob/ob* macrophages, IL-6 levels are higher after LPS treatment compared with WT but followed a trend similar to that of BMDMs from WT mice (Supplementary Fig. 1*A*). Thus, leptin signaling through ObR is sufficient to enhance the production of proinflammatory cytokines in activated macrophages.

We next evaluated real-time metabolic changes in leptin-treated macrophages. We found that leptin exacerbates LPS-induced glycolysis, observed with ECAR, which was maintained even after macrophages were submitted to a glycolytic stress test (Fig. 1*C* and *D*). Leptin had no additive effect on LPS-induced blockade of oxygen consumption by macrophages (Fig. 1*E* and *F*). We next investigated whether the inflammatory effects of leptin in macrophages are dependent on glucose metabolism. We used an approach of energetic carbon source limitation. We cultivated macrophages in complete media, glucose-free media + galactose, or glucose-free media (PBS) for 6 h. This enables us to determine the importance of glycolysis to the inflammatory response. For galactose to enter the glycolytic pathway, there is energetic involvement in the form of two UDP-dependent reactions (galactose 1 phosphate formation and epimerization of UDP-galactose) (29–31). We found that the additive effect of leptin in LPS-activated macrophages was lost in glucose-deprived conditions (Gal and PBS), as measured by TNF-α and IL-6 (Fig. 1*G*). Thus, leptin activity in macrophages requires biomolecules generated by glucose metabolism to fuel its downstream pathways and promote inflammation. Next, we determined the significance of metabolic alterations to the function of leptin-treated macrophages. We did a pharmacological inhibition of lactate dehydrogenase (LDH) using oxamate (OXA) and observed that BMDM failed to induce leptin-dependent cytokine expression (*Il6*) on oxamate treatment, with no changes in *Tnfα* expression levels (Supplementary Fig. 1*D*). Our results show that LDH activity is essential for leptin-dependent booster in LPS-induced proinflammatory cytokine expression. We then pharmacologically inhibited mitochondrial pyruvate carrier with UK-5099, preventing pyruvate entry into mitochondria without affecting glycolysis. UK-5099 treatment did not have the same inhibitory effect in proinflammatory cytokine expression triggered by leptin in LPS-activated macrophages as observed with OXA (Supplementary Fig. 1*E*). Thus, pyruvate entry, and its subsequent oxidation in mitochondria, is not necessary for leptin-induced booster of proinflammatory cytokine expression on LPS activation. Together, these results indicate that glycolysis, but not mitochondrial metabolism, is important for leptin effects in activated proinflammatory macrophages.

During the metabolic adaptation, LPS-activated macrophages shut down fatty acid oxidation and present breaks in the tricarboxylic acid cycle that allow the accumulation of succinate and citrate and production of itaconate (15,32). Using ^{13}C glucose, we did not observe further

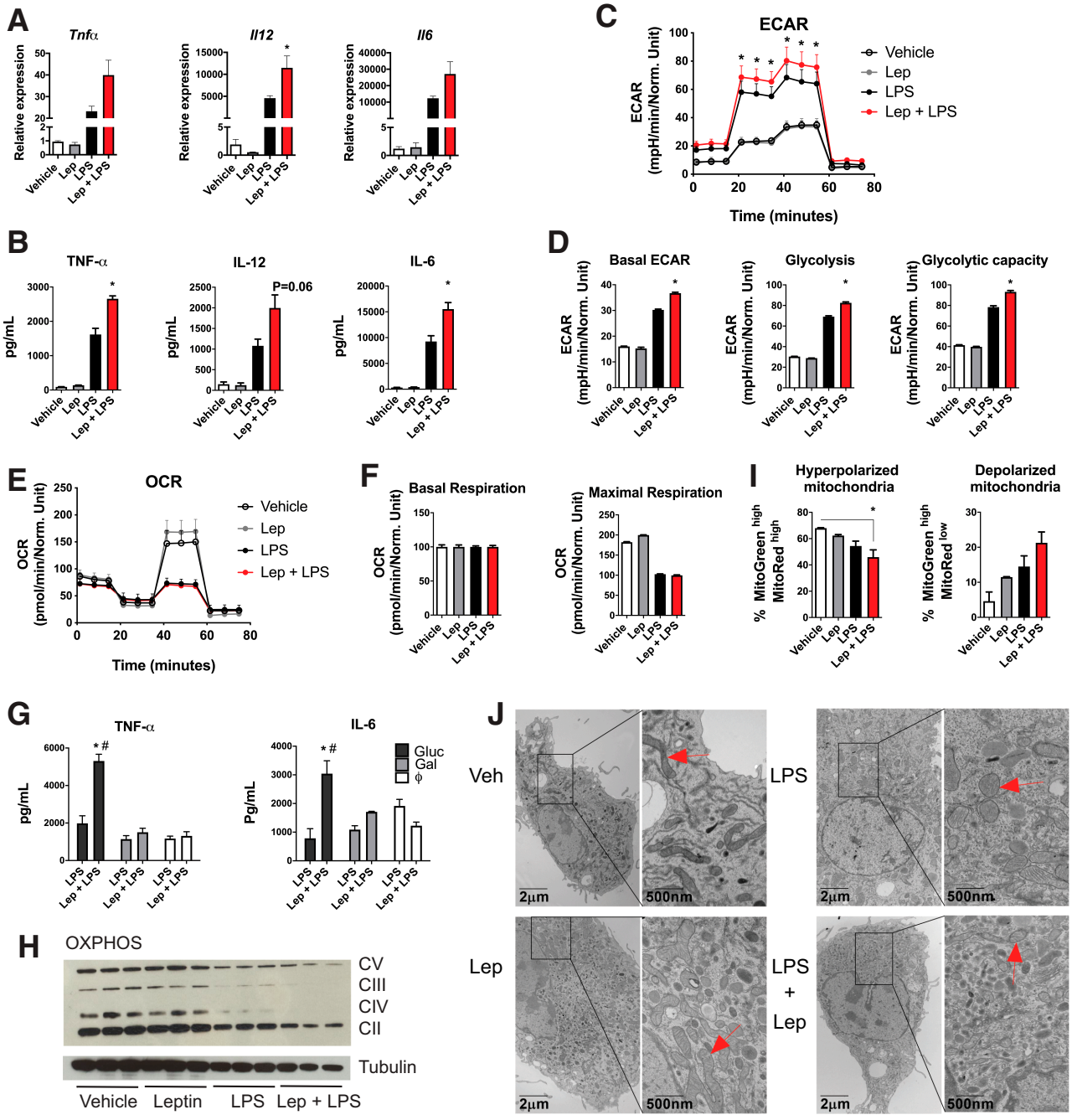

Figure 1—Leptin potentiates LPS-induced metabolic reprogramming in macrophages. BMDM were pretreated with leptin (Lep) (100 ng/mL) for 30 min and activated with LPS (100 ng/mL) for 6 hours. *A*: Relative mRNA expression of proinflammatory cytokines (*Tnfα*, *Il6*, and *Il12)* by qPCR. *B*: Proinflammatory cytokines levels (TNF-α, IL-6, and IL-12) in the supernatant of activated BMDMs by ELISA. *C*: ECAR of macrophages on glycolytic stress (injections of glucose, oligomycin, and 2-deoxyglucose). *D*: Basal ECAR levels, ECAR analysis of glycolysis (followed by glucose injection), and glycolytic capacity (followed by oligomycin injection). *E*: OCR of macrophages on mitochondrial stress test (injections of oligomycin, FCCP, antimycin, and rotenone). *F*: OCR analysis of basal respiration and maximal respiration (followed by FCCP injection). *G*: BMDMs were cultured in complete media (Gluc), glucose-free media + galactose 500 μmol/L (Gal), or glucose-free media (PBS) and treated with leptin and/or LPS for 6 hours. Concentration of proinflammatory cytokine levels (TNF-α and IL-6) in the supernatant by ELISA. *H*: Total content of subunits representing OXPHOS protein complexes (CV, CIII, CIV, CII) were measured with Western blot. *I*: Analysis of mitochondrial function with MitoTracker Green and MitoTracker Red after 6 h of activation. Polarized mitochondria (MitoGreen^{high} MitoRed^{high}) and depolarized mitochondria (MitoGreen^{high} MitoRed^{low}). *J*: Electron mycroscopy of BMDMs after 6 h of activation (leptin/LPS). Red arrows indicate mitochondria. Data are means ± SEM. $n = 3/5$ per group. One-way ANOVA with Bonferroni multiple comparison test (*A–F*). $*P < 0.05$, $\#P < 0.05$ compared with all groups. *A–F* and *I* are representative of three independent experiments. *G*, *H*, and *J* are representative of two experiments. Norm., normalized units.

carbon incorporation into citrate and itaconate by leptin in relation to LPS-activated macrophages (Supplementary Fig. 1*F* and *G*). This indicates that the metabolic rewiring promoted by LPS is sufficient to induce increased cytokine production through stimulation with leptin even without additive effects on the inhibition of oxygen consumption and alterations in the tricarboxylic acid cycle. However, because changes in glycolytic rates are related to mitochondrial modulation, we next analyzed the contents of subunits representing the electron transport chain (ETC) mitochondrial complexes and observed that LPS-induced reduction in ETC complexes is exacerbated by cotreatment with leptin (Fig. 1*H*). We then investigated the mitochondrial membrane potential in leptin-treated macrophages, since mitochondrial polarization can reflect the functionality of the ETC. Analysis of mitochondrial phenotype using the probes MitoTracker Green and Red revealed an increase in depolarized mitochondria (MitoGreen^{high} MitoRed^{low}), whereas hyperpolarized mitochondria (MitoGreen^{high} MitoRed^{high}) were decreased in leptin-treated macrophages (Fig. 1*I*), even though the total mitochondrial mass remained equivalent (Supplementary Fig. 1*H*). Moreover, ultrastructural analysis showed that, consistent with elevated ECAR and reduced levels of mitochondrial ETC complexes, LPS and leptin cotreated macrophages display enhanced alterations in mitochondria morphology, observed as short and rounded mitochondria with looser cristae (Fig. 1*J*). These results indicate that leptin contributes to the inflammatory phenotype through potentiation of LPS effects on mitochondrial morphology and function, and glucose-dependent metabolism.

Leptin Effects in Macrophages Depend on mTOR Activation

Leptin signaling in macrophages increases LPS-induced cytokine release through metabolic changes. We used the Cre-lox system to generate mice with a specific deletion of ObR in myeloid cells. We used ObR floxed (ObR$^{fl/fl}$) and LysM^{Cre} mice to study macrophages lacking leptin signaling. Consistent with what we observed from *db/db* mice, mice with conditional deletion of leptin receptor (ObR$^{-/-}$) in macrophages fail to enhance LPS-induced expression and secretion of proinflammatory cytokines (TNF-α, IL-12, IL-6) compared with control (ObR$^{fl/fl}$) (Fig. 2*A* and *B*). We also analyzed the percentage of TNF-α–positive and IL-12–positive macrophages and IL-6 secretion in LPS-activated macrophages from both ObR$^{fl/fl}$ and ObR$^{-/-}$ mice and found that lack of leptin receptor impaired the enhanced production and secretion of TNF-α, IL-12, and IL-6 in response to leptin plus LPS (Fig. 2*B* and *C* and Supplementary Fig. 2*A*).

To determine the relevance of signaling pathways responsible for leptin-mediated effects on macrophages, we analyzed the downstream activation of mTOR by leptin. We observed that leptin induced the phosphorylation of both mTORC1 and mTORC2 downstream targets, 4EBP1 and AKT^{Ser473}, respectively (Fig. 2*D*). Cotreatment with leptin and LPS sustained the phosphorylation of AKT^{Ser473} rather than 4EBP1 (Fig. 2*D*). We also found that S6 kinase, an mTORC1 target, is phosphorylated on LPS activation, whereas cotreatment with leptin did not alter the signal intensity, showing that LPS-induced mTORC1 activation was not magnified by leptin (Supplementary Fig. 2*B*). Rapamycin is a potent mTOR inhibitor that when administered at higher doses inhibits both complexes of mTOR (mTORC1 and mTORC2) (33–36). We treated macrophages with 200 nmol/L of rapamycin for 20 min before activating the cells with leptin/LPS to inhibit both mTORC1 and mTORC2 pathways. Rapamycin-treated cells displayed reduced phosphorylation of 4EBP1 and AKT^{Ser473}, indicating inhibition of both mTORC1 and mTORC2 (Fig. 2*D*). Thus, mTOR complexes are differentially activated by leptin after LPS treatment.

Next, we determined the effect of rapamycin treatment on leptin-mediated cytokine secretion in activated macrophages. Rapamycin also limited the exacerbated cytokine production by macrophages cotreated with leptin and LPS, reducing the levels of cytokines back to those induced by LPS alone (TNF-α and IL-12) and even to control levels (IL-6) (Fig. 2*E*). To determine whether mTOR participates in leptin-induced metabolic adaptation of macrophages, we also treated BMDMs with rapamycin prior to activation with leptin and LPS and submitted the cells to a glycolytic stress test. We found that mTOR signaling is necessary for the leptin-dependent booster in glycolytic capacity (Fig. 2*F*). The STAT3 pathway can also be triggered by leptin. Next, we investigated the contribution of the STAT3 pathway for leptin effects on macrophages. First, we used shRNA to target STAT3 (shSTAT3). We confirmed STAT3 knockdown in BMDM prior to the experiments (Supplementary Fig. 2*C*). Leptin-dependent booster of LPS-induced *Tnfα* expression still occurred in STAT3-deficient macrophages. (Supplementary Fig. 2*C*). Together, these results indicate that leptin-induced mTOR activation, and not the activation of STAT3 pathway, is necessary for leptin-mediated effects on LPS-activated macrophages.

To better understand the role of each mTOR complex in leptin-induced macrophage activation, we crossed Rictor and Raptor floxed mice (Rictor$^{fl/fl}$ and Raptor$^{fl/fl}$) with LysM^{Cre} mice to generate macrophages lacking mTORC2 and mTORC1 activity, respectively. Rictor and Raptor are scaffold proteins that integrate mTORC2 and mTORC1 complexes, and they are necessary for the complex to be functional (37). TNF-α and IL-6 levels were significantly reduced in leptin/LPS-treated macrophages derived from Rictor knockout (Rictor$^{-/-}$) mice compared with control Rictor$^{fl/fl}$ (Fig. 2*G*), which was similar to what we observed in ObR$^{-/-}$ macrophages (Fig. 2*A*–*C*). We did not observe a significant difference in TNF-α and IL-6 concentration in the supernatant of either Raptor$^{-/-}$ or Raptor$^{fl/fl}$ control macrophages after LPS and leptin plus LPS treatments (Fig. 2*H*). Together, our data indicate that mTOR activity

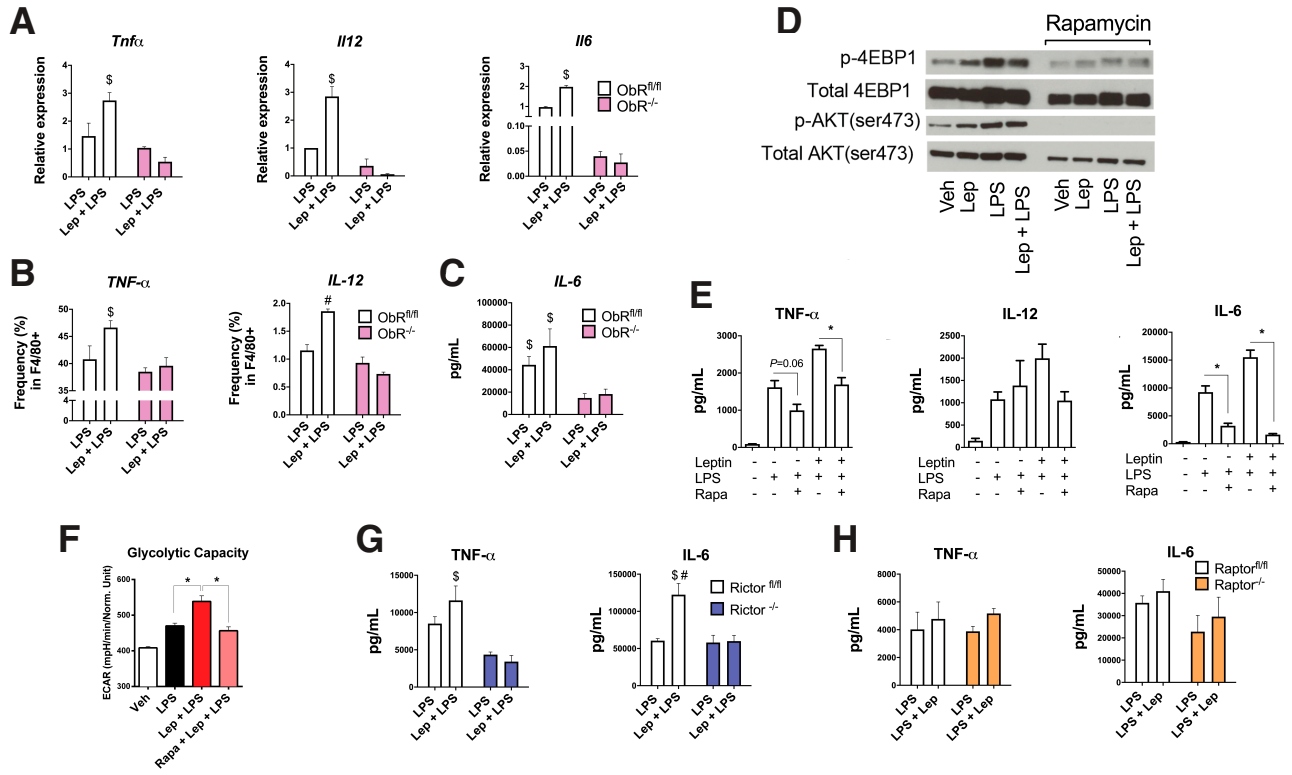

Figure 2—Effects of leptin (Lep) on macrophages depend on mTOR activation. *A*: Relative mRNA expression of *Tnfα*, *Il6*, and *Il12* from $ObR^{fl/fl}$ and $ObR^{-/-}$ mice after 6 h activation with leptin/LPS (100 ng/mL). *B*: TNF-α– and IL-12–positive macrophages from $ObR^{fl/fl}$ and $ObR^{-/-}$ mice after 6 h of activation with leptin/LPS were measured by flow cytometry. *C*: Concentration of IL-6 in the supernatant of leptin/LPS-activated BMDMs from $ObR^{fl/fl}$ and $ObR^{-/-}$ mice was measured with ELISA. *D*: BMDMs were pretreated with rapamycin (200 nmol/L) for 15 min and then activated with leptin/LPS for 15 minutes. Total and phosphorylated content of 4EBP1 and AKT^{Ser473} was measured by Western blot. Veh, vehicle. *E*: BMDMs from WT mice were pretreated with rapamycin (Rapa) (200 nmol/L) for 20 min and then activated with leptin/LPS for 6 h. Concentration of TNF-α, IL-6, and IL-12 in the supernatant was measured by ELISA. *F*: ECAR analysis of glycolysis (followed by glucose injection) in BMDMs treated with rapamycin (20 nmol/L) for 20 min and then activated with leptin/LPS for 6 h. *G*: Concentration of TNF-α and IL-6 in the supernatant of BMDMs activated for 6 h with leptin/LPS from $Rictor^{fl/fl}$ and $Rictor^{-/-}$ mice was measured with ELISA. *H*: Concentration of TNF-α and IL-6 in the supernatant of leptin/LPS-activated BMDMs from $Raptor^{fl/fl}$ and $Raptor^{-/-}$ mice was measured with ELISA. Data are means ± SEM. $n = 3/5$ per group. One-way ANOVA with Bonferroni multiple comparison test (*A–C* and *E*) $^*P < 0.05$, $\#P < 0.05$ compared with all groups; $\$P < 0.05$ $ObR^{fl/fl}$ vs. $ObR^{-/-}$. *A–C* and *F–H* are representative of three independent experiments, and *D* and *E* are representative of two independent experiments. γ, M1 polarization. Norm., normalized units.

fuels the exacerbated inflammatory response mediated by leptin, specifically, through the mTORC2 pathway.

Next, we characterized the role of leptin signaling in macrophages in an in vitro condition of disrupted metabolic homeostasis to mimic what happens in vivo during obesity. We performed in vitro metabolic activation (Mme) of macrophages (addition of glucose 30 mmol/L, insulin 10 nmol/L, and palmitate 0.4 mmol/L) as previously described (38). We found that the lack of leptin signaling in Mme macrophages increased the expression of the M2-related markers *Il10* and *Mrc1* (Supplementary Fig. 2*D*). However, as the mice gain weight, other systemic factors enable an accentuated inflammatory environment. In this context, leptin favors the proinflammatory phenotype. We also observed that Mme macrophages from $ObR^{-/-}$ mice displayed increased expression of lipid metabolism markers *Cd36* and *Abca1* with no effect on *Plin2* (Supplementary Fig. 2*E*). This suggests that the macrophages become dysregulated and the loss of leptin signaling indulges the dysfunctional response.

Leptin Alters IL-4–Treated Macrophage Metabolism

Considering the importance of mTORC2 for the differentiation of M2-like macrophages (IL-4) (39) and that mTORC2 is necessary for the effects of leptin in activated macrophages, we hypothesized that leptin may act as a systemic nutritional status signaling molecule to modulate macrophage phenotype regardless of their inflammatory milieu, since both classical and alternative macrophage activation processes are energy demanding. Thus, we polarized macrophages into a proinflammatory (IFN-γ + LPS)-like or repair (IL-4)-like profile. Using leptin receptor reporter mice, we observed that IL-4–treated macrophages [M(IL-4)] showed increased ObR expression in comparison with

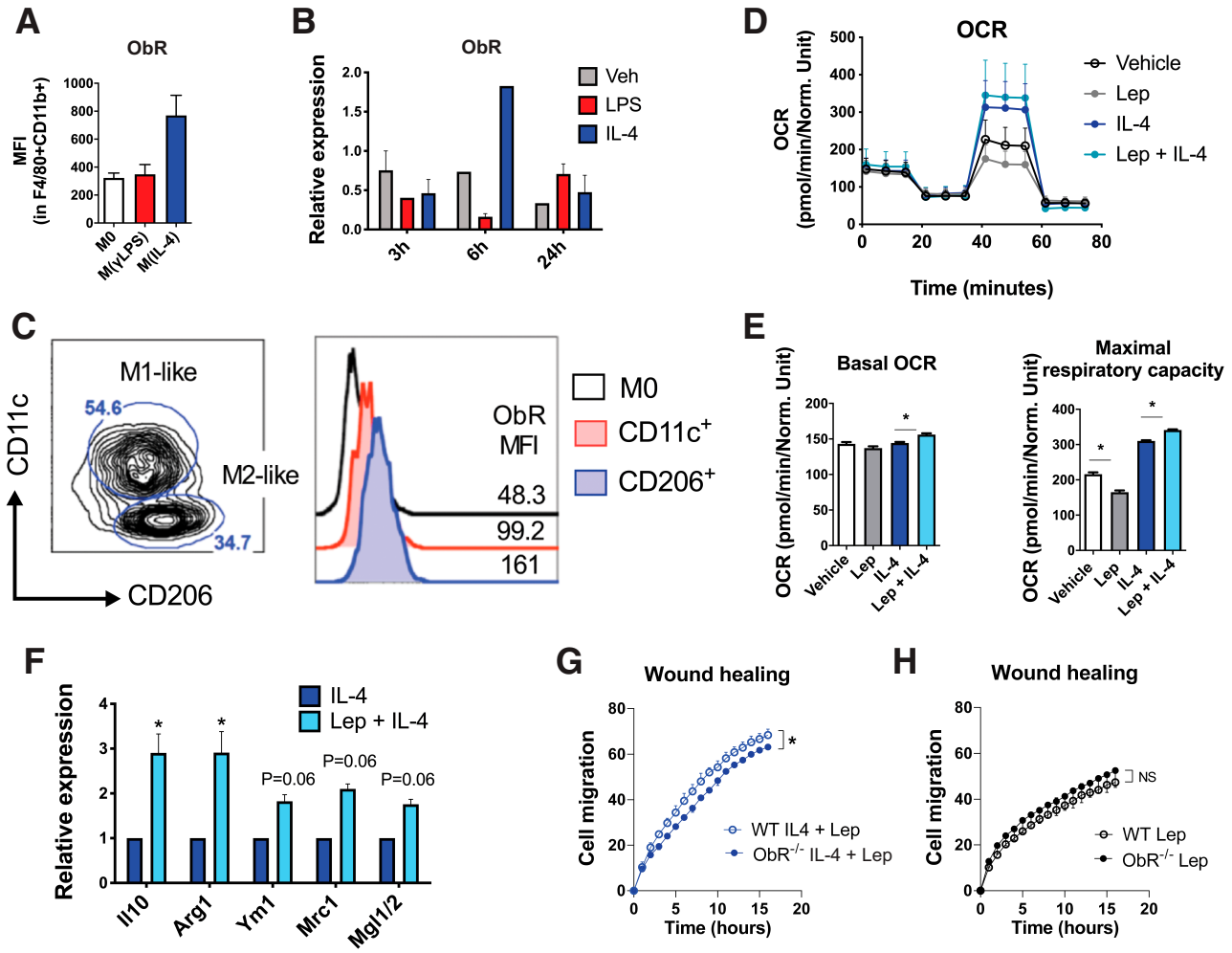

Figure 3—Leptin (Lep) alters M(IL-4) metabolism and function. *A*: Median fluorescence intensities (MFI) of ObR expression in BMDMs from WT mice stimulated with LPS (100 ng/mL) + IFN-γ (20 ng/mL) or IL-4 (20 ng/mL) for 24 h were measured by flow cytometry. *B*: Relative gene expression of ObR in WT BMDMs treated with LPS (100 ng/mL) or IL-4 (20 ng/mL) for 3, 6, and 24 h was measured with qPCR. Veh, vehicle. *C*: Representative histogram of ObR expression (median fluorescence intensity) from $CD11c^+$ and $CD206^+$ ATMs isolated from ObR reporter mice was obtained with flow cytometry. *D*: OCR of macrophages on mitochondrial stress test (injections of oligomycin, FCCP, antimycin, and rotenone). *E*: OCR analysis of basal respiration and maximal respiration (followed by FCCP injection). *F*: Relative gene expression of *Arg1*, *Mrc1*, *Il10*, *Ym1*, and *Mgl* by qPCR from BMDMs treated with IL-4/leptin for 24 h. *G*: Cell migration toward the wound site by M(IL-4) from WT and $ObR^{-/-}$ mice. *H*: Cell migration toward the wound site by BMDMs from WT and $ObR^{-/-}$ mice. Data are mean ± SEM. *n*= 3/5 per group. One-way ANOVA with Bonferroni multiple comparisons test. $*P < 0.05$. *A–C* are representative of two independent experiments. *D–H* are representative of three independent experiments. γ, M1 polarization. Norm., normalized units.

resting (M0) and proinflammatory [M(IFN-γ + LPS)] macrophages (Fig. 3*A*). We also performed a time course analysis of ObR expression in macrophages treated with either IL-4 or LPS for 3, 6, and 24 h. We found that M(IL-4) express the highest levels of ObR 6 h after the stimulus (Fig. 3*B*). Next, we isolated ATMs from ObR reporter mice and determined ObR expression in $CD11c^+$ and $CD206^+$ macrophages. CD11c is expressed predominantly in proinflammatory ATMs and CD206 in tissue-resident/anti-inflammatory ATMs (8,12,40). Similar profile was observed in ATMs, where $CD206^+$ macrophages showed the highest ObR levels (Fig. 3*C*).

We then hypothesized that M(IL-4) would also be susceptible to leptin-induced metabolic adaptations, due to the elevated ObR expression. We analyzed the total glucose, lactate, and glutamine contents in the supernatant of M(IL-4) and observed a reduction in glucose concentration, indicating higher glucose consumption by these cells (Supplementary Fig. 3*A*), with no change in lactate and glutamine levels (Supplementary Fig. 3*A*). We observed that cotreatment with leptin and IL-4 enhanced IL-4–mediated reduction of glycolysis and glycolytic capacity and increased OCR and maximal respiratory capacity (Fig. 3*D and E* and Supplementary Fig. 3*B* and *C*). We next analyzed the expression of a series of alternatively activated macrophage markers (*Arg1*, *Mrc1*, *Il10*, *Ym1*, *Mgl1/2*). We observed that leptin boosted the expression of all M (IL-4)-associated markers (Fig. 3*F*). We then performed

a real-time migration assay to assess the role of leptin in an in vitro model of macrophage-induced tissue repair, which enables us to determine the function of IL-4–polarized macrophages. We observed that loss of leptin signaling in M(IL-4) reduces macrophage migration into the wound site (Fig. 3*G*). We also showed that this is context dependent, since in the absence of IL-4 stimulus, leptin does not affect cell migration, as observed in the same migration rates in the WT and $ObR^{-/-}$ BMDM (Fig. 3*H*). Thus, following along with our hypothesis, leptin cannot enhance the repair phenotype by itself, but when macrophages are primed with IL-4 and potentially in an IL-4–rich microenvironment, leptin signaling boosts the tissue repair phenotype. Together, our data show that leptin functions as a checkpoint to boost macrophage activation and polarization, amplifying metabolic and immunologic alterations to support the desired phenotype for which macrophages have been primed.

Finally, to better understand the role of mTOR in M(IL-4) metabolic adaptation, we submitted BMDMs from WT, $Rictor^{-/-}$, and $Raptor^{-/-}$ mice to a Mito Stress Test. Raptor-deficient BMDMs showed lower OCR, as well as ECAR, compared with WT (Supplementary Fig. 3*D* and *E*). Maximal respiration was partially restored by leptin treatment in $Raptor^{-/-}$ cells, albeit still reduced in comparison with control (Supplementary Fig. 3*F*). On IL-4 treatment, we observed that Raptor deletion inhibited glycolysis in macrophages, which was not affected by leptin treatment (Supplementary Fig. 3*D*). We also observed that, much like Raptor-deficient BMDM, $Rictor^{-/-}$ macrophages also have lower metabolic rates, as characterized by OCR and ECAR (Fig. 3*G* and *H*). Moreover, we analyzed the importance of STAT3 in leptin-dependent increase in the expression of M2 marker *Mrc1*. We found that loss of STAT3 signaling on M(IL-4) reduced the expression of *Mrc1* in comparison with control shGFP. However, leptin-mediated booster of *Mrc1* in shSTAT3 BMDMs remained intact (Supplementary Fig. 3*I*). This highlights the importance of mTOR activity to optimal cellular function, since macrophages adapt their metabolism during the differentiation process. mTOR is necessary for the metabolic reprogramming during IL-4 activation (39). We suggest that leptin acts, at least in part, in a mechanism that is independent of mTORC1 but dependent on mTORC2 to compensate for the energetic demand in M(IL-4).

Loss of Leptin Signaling in Myeloid Cells Improves Glucose Tolerance in Obese Mice

Because obesity is associated with changes in macrophage phenotype, we used a model of diet-induced obesity, which also leads to hyperleptinemia and inflammation (41). This is an excellent model where macrophage phenotype and increased leptin levels can be analyzed simultaneously in vivo. Because leptin enhances both proinflammatory macrophage activation and tissue repair/anti-inflammatory profile in vitro and both leptin and proinflammatory macrophages are increased in the AT of obese people and mice, we hypothesized that inhibition of leptin signaling on macrophages could directly impact systemic low-grade inflammation and the subsequent insulin resistance. We first submitted $ObR^{-/-}$ mice to HFD. Control ($ObR^{fl/fl}$) and $ObR^{-/-}$ mice had no changes in body weight or weight gain (Supplementary Fig. 4*A*). Next, we analyzed systemic insulin resistance and glucose tolerance. $ObR^{-/-}$ mice showed improved glucose tolerance compared with control $ObR^{fl/fl}$, as shown by faster reduction in blood glucose levels and reduced area under the curve (Fig. 4*A* and *B*). $ObR^{-/-}$ mice also displayed improved insulin sensitivity on HFD feeding (Fig. 4*C* and *D*). When fed a normal diet, $ObR^{fl/fl}$ and $ObR^{-/-}$ mice showed similar glucose tolerance and insulin sensitivity (Supplementary Fig. 4*B–E*). Moreover, we observe that in both $ObR^{fl/fl}$ and $ObR^{-/-}$ mice, basal glucose levels in the serum are not different after 5 h or 12 h of fasting (Supplementary Fig. 4*F*). Only after hyperglycemic stress (GTT) were we able to determine the faster recovery $ObR^{-/-}$ HFD-fed mice (Fig. 4*A*). Glucose and cholesterol levels increase in both $ObR^{fl/fl}$ and $ObR^{-/-}$ HFD-fed mice under nonfasting conditions and cholesterol levels are decreased in HFD $ObR^{-/-}$ mice in comparison with WT HFD-fed mice (Supplementary Fig. 4*G*). This suggests that loss of leptin signaling in myeloid cells of obese mice is important to improve systemic glucose homeostasis, as observed when mice were submitted to a stress test (GTT and ITT). Thus, impairment of leptin signaling in myeloid cells is sufficient to improve systemic metabolic impairment caused by HFD feeding.

Because inflammation has a causative role in obesity-induced insulin resistance (12,42), we evaluated the macrophage phenotype in lean and obese $ObR^{fl/fl}$ and $ObR^{-/-}$ mice. There were no significant differences in the production of proinflammatory cytokines by ATMs isolated from pgAT of obese $ObR^{fl/fl}$ and $ObR^{-/-}$ mice (Fig. 4*E*). However, pMacs from $ObR^{-/-}$ mice produced lower levels of IL-6 and IL-1β compared with control ($ObR^{fl/fl}$) and similar levels of TNF-α (Fig. 4*F*), which can directly contribute to systemic low-grade inflammation (9). ATMs and pMacs from chow-fed $ObR^{fl/fl}$ and $ObR^{-/-}$ mice produced similar levels of proinflammatory cytokines (Supplementary Fig. 4*I–J*).

We analyzed the expression of proinflammatory (M1) markers and repair (M2) markers in both ATMs and pMacs of $ObR^{fl/fl}$ and $ObR^{-/-}$ mice. We found that, in ATMs, the frequency of proinflammatory $CD11c^{+}$ cells increases when both $ObR^{fl/fl}$ and $ObR^{-/-}$ mice are fed an HFD (Fig. 4*G*). Interestingly, though, the frequency of M2/repair-related marker CD206 is only decreased after HFD in ATMs of $ObR^{fl/fl}$ mice (Fig. 4*G*). $ObR^{-/-}$ mice maintained a similar frequency of $CD206^{+}$ ATMs during

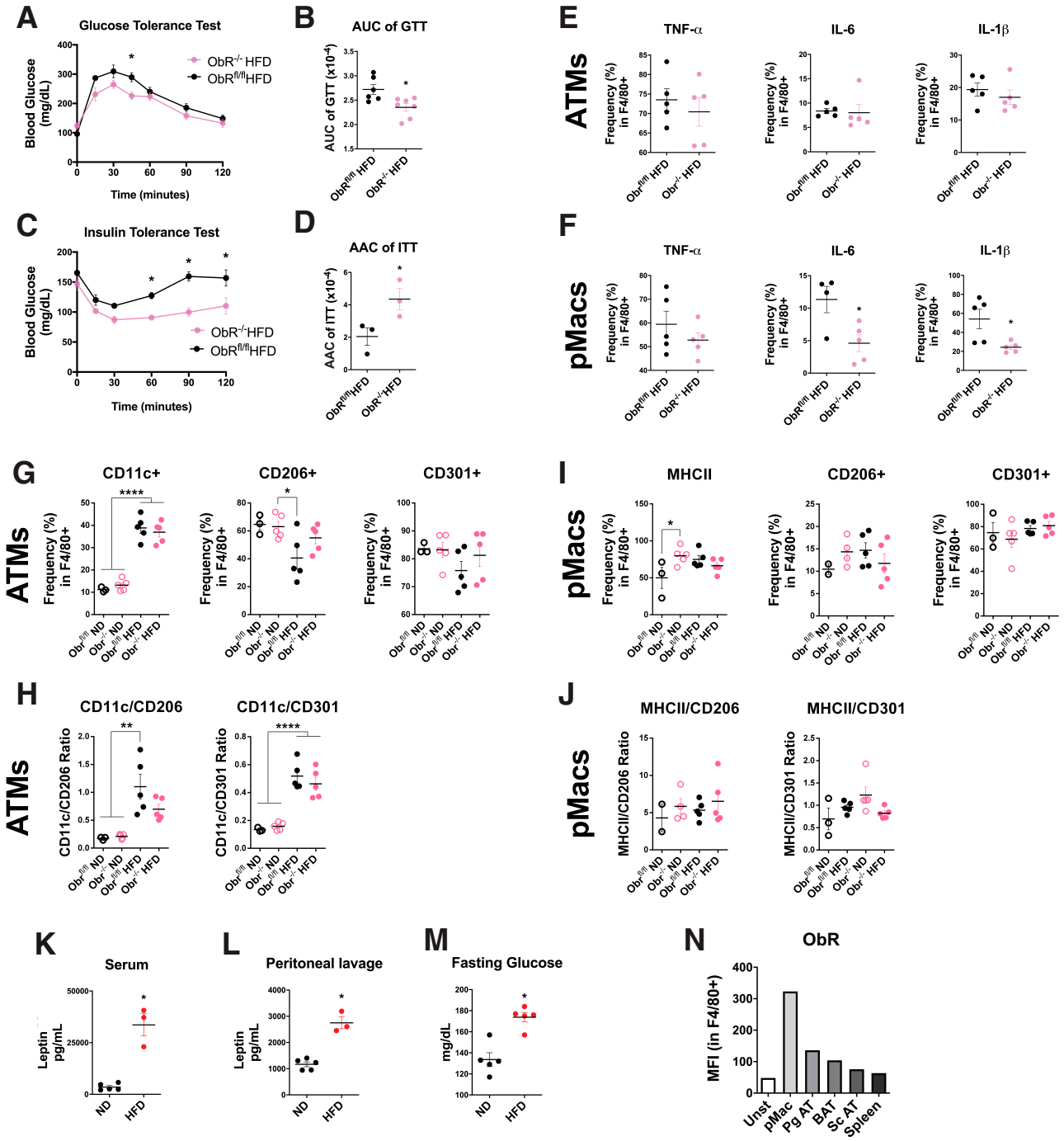

Figure 4—Loss of leptin signaling in myeloid cells ameliorates insulin resistance in obese mice. *A*: GTT in HFD-fed ObR$^{fl/fl}$ and ObR$^{-/-}$ mice. *B*: Area under the curve (AUC) of GTT in HFD-fed ObR$^{fl/fl}$ and ObR$^{-/-}$ mice. *C*: ITT in HFD-fed ObR$^{fl/fl}$ and ObR$^{-/-}$ mice. *D*: Area above the curve (AAC) of ITT test in HFD-fed ObR$^{fl/fl}$ and ObR$^{-/-}$ mice. *E*: Frequency of IL-6–, IL-1β–, and TNF-α–positive macrophages (F4/80^{+}) from the AT of HFD-fed ObR$^{fl/fl}$ and ObR$^{-/-}$ mice. *F*: Frequency of IL-6–, IL-1β–, and TNF-α–positive macrophages (F4/80^{+}) from the peritoneal lavage of HFD-fed ObR$^{fl/fl}$ and ObR$^{-/-}$ mice. *G*: Frequency of CD11c-, CD206-, and CD301-positive macrophages (F4/80^{+}) from the AT of ND- and HFD-fed ObR$^{fl/fl}$ and ObR$^{-/-}$ mice. *H*: Ratio of CD11c-positive to CD206-positive and CD11c-positive to CD301-positive macrophages (F4/80^{+}) from the AT of ND- and HFD-fed ObR$^{fl/fl}$ and ObR$^{-/-}$ mice. *I*: Frequency of MHCII-, CD206-, and CD301-positive macrophages (F4/80^{+}) from the peritoneal lavage of ND- and HFD-fed ObR$^{fl/fl}$ and ObR$^{-/-}$ mice. *J*: Ratio of MHCII-positive to CD206-positive and MHCII-positive by CD301-positive macrophages (F4/80^{+}) from the peritoneal lavage of ND- and HFD-fed ObR$^{fl/fl}$ and ObR$^{-/-}$ mice. *K*: Leptin concentration in the serum of chow-fed (ND) and HFD-fed mice. *L*: Leptin concentration in the peritoneal lavage of ND-fed and HFD-fed mice. *M*: Glucose levels in the serum of chow-fed (ND) and HFD-fed mice after 5 h of fasting. *N*: Median fluorescence intensity (MFI) of ObR in macrophages from different tissues: peritoneal lavage (pMacs), pgAT, brown AT (BAT), subcutaneous AT (Sc AT), spleen, and the unstained control (Unst). Data are means ± SEM. $n = 3/5$ per group. *A* and *C*: Two-way ANOVA Sidak multiple comparison test. *B*, *D–F*, and *K–M*: Unpaired two-tailed Student *t* test. *$P < 0.05$. *A–D* and *G–I* representative of three independent experiments. *E–J* and *N* are representative of two independent experiments.

normal diet (ND) and HFD feeding (Fig. 4*G*). This affects the ratio of proinflammatory to repair types of macrophages, where the CD11c-to-206 ratio is elevated in $ObR^{fl/fl}$ mice after HFD but not in $ObR^{-/-}$ mice (Fig. 4*H*). We observed no significant changes in the frequency of $CD301^+$ ATMs between the groups (Fig. 4*G* and *H*). The CD11c-to-CD301 ratio was higher in both $ObR^{fl/fl}$ and $ObR^{-/-}$ mice after HFD (Fig. 4*H*). In pMacs, we found an increase in MHCII in $ObR^{-/-}$ mice even during ND, but no other significant changes were observed regarding the frequency of $CD206^+$ or $CD301^+$ pMacs between the groups (Fig. 4*I*). There were also no significant changes in the ratios of MHCII to CD206 or MHCII to 301 pMacs on either diet (Fig. 4*J*). Our data highlight how differently these macrophages respond to nutritional alterations. The lack of leptin receptor prevents the raise in proinflammatory-to-repair ratio caused by HFD feeding, which agrees with our data that show no significant increases in the expression of proinflammatory cytokines (TNF-α, IL-6, IL-1β) in ATMs of $ObR^{-/-}$ obese mice.

Next, we aimed to determine the mechanisms by which ATMs and pMacs from obese mice respond differentially. We submitted WT mice to HFD feeding for 8 weeks. HFD-fed mice presented increased weight gain, elevated fasting glucose, and elevated levels of leptin both in serum and peritoneal lavage (Fig. 4*K*–*M*). We then assessed the pattern of ObR expression in vivo from macrophages of various tissues. Using ObR reporter mice, we found that pMacs express the highest levels of ObR compared with other tissue-resident macrophages, such as ATMs from pgAT, brown AT, subcutaneous AT, and splenic macrophages (Fig. 4*N*). The expression of ObR in pMacs and ATMs was also not affected by HFD (Supplementary Fig. 4*K*). Thus, ObR expression in these tissue-resident macrophages seems to be modulated by the microenvironment in which they reside. In the obese AT, macrophages are exposed to leptin in high concentrations, whereas the peritoneal cavity is not rich in leptin. Accordingly, the levels of leptin in the peritoneal cavity are ∼10 times lower than in the blood (peritoneal cavity, lean mean ± SEM 1,167 ± 93.64, obese 2,749 ± 225.7; serum, lean 3,518 ± 728.9, obese 33,629 ± 5,395) (Fig. 4*K* and *L*). Thus, the reduced expression of ObR in ATMs may prevent hyperresponsiveness to leptin in AT. It is likely that pMacs are more prone to intensify leptin responses because of higher expression of ObR, since this intensified response is abolished in $ObR^{-/-}$ mice (Fig. 4*N*). Once again, these data highlight the importance of ObR expression in pMacs and the subsequent activation of mTOR by leptin to promote functional changes even if the macrophage phenotype remains similar. Our results indicate that blocking leptin signaling ($ObR^{-/-}$) in myeloid cells ameliorates systemic glucose homeostasis and inflammation in obesity.

ATMs and pMacs Display Distinct mTOR Activation in Obesity

The expression of leptin receptor in pMacs and ATMs and the levels of leptin in the microenvironment where these cells reside suggest that they may respond differentially to leptin signaling, which could directly impact their responsiveness to an inflammatory stimulus. Our next step was to evaluate the activity of mTOR complexes in vivo in conditions where leptin levels are increased, such as during obesity. We submitted mice to HFD and isolated pgAT and pMacs from both lean and obese mice (Supplementary Fig. 5*A*) and analyzed cytokine production as a readout of the obesity-induced inflammatory state. We observed elevated cytokine production in ATMs (TNF-α) and pMacs (TNF-α and IL-6) of obese hyperleptinemic mice (Fig. 5*A* and *B*), consistent with our in vitro data. We also selected $CD206^+$ ATMs and pMacs and noticed that in ATMs, only IL-6 was increased during HFD feeding, whereas $CD206^+$ pMacs showed elevated levels of both TNF-α and IL-6 (Supplementary Fig. 5*B* and *C*). Next, we analyzed the phosphorylation of STAT3, of S6 kinase, and of AKT^{Ser473} in ATMs and pMacs. Both ATMs and pMacs from HFD-fed mice presented higher levels of phosphorylated STAT3 (p-STAT3), as a possible consequence of hyperleptinemia and intense leptin signaling in these macrophages (Fig. 5*C* and *D*). However, ATMs and pMacs showed a distinct mTOR activation pattern. The phosphorylation of S6 kinase and AKT^{Ser473} (p-S6 and p-AKT, respectively) was diminished in ATMs and increased in pMacs (Fig. 5*C* and *D*). A similar pattern was found in $CD206^+$ macrophages from the pgAT and peritoneal lavage of obese mice (Supplementary Fig. 5*D* and *E*). These results indicate that leptin levels in the microenvironment and ObR expression in tissue-resident macrophages affect the activation of the mTOR pathway in a tissue-specific manner during obesity.

DISCUSSION

The contribution of immune cells to obesity-related inflammation has been extensively reported (43,44). Leptin deficiency promotes an anti-inflammatory profile in mast cells, which improves obesity and insulin resistance in mice (45). Even though hyperleptinemia contributes to low-grade systemic inflammation, it is still not entirely clear how leptin modulates macrophage inflammation in vivo. Here, we showed by genetic deletion of ObR in myeloid cells that blocking leptin signaling in macrophages is sufficient to improve glucose tolerance and insulin sensitivity in obese mice. We also showed that pMacs play a key role increasing systemic inflammation because of their phenotypical features, which include high expression of ObR, elevated response to leptin, and increased expression of proinflammatory cytokines. Our work highlights the role of leptin signaling in tissue-resident macrophages in obesity and the differential contribution of mTOR complexes to the hyperinflammatory response. Moreover, we propose the concept

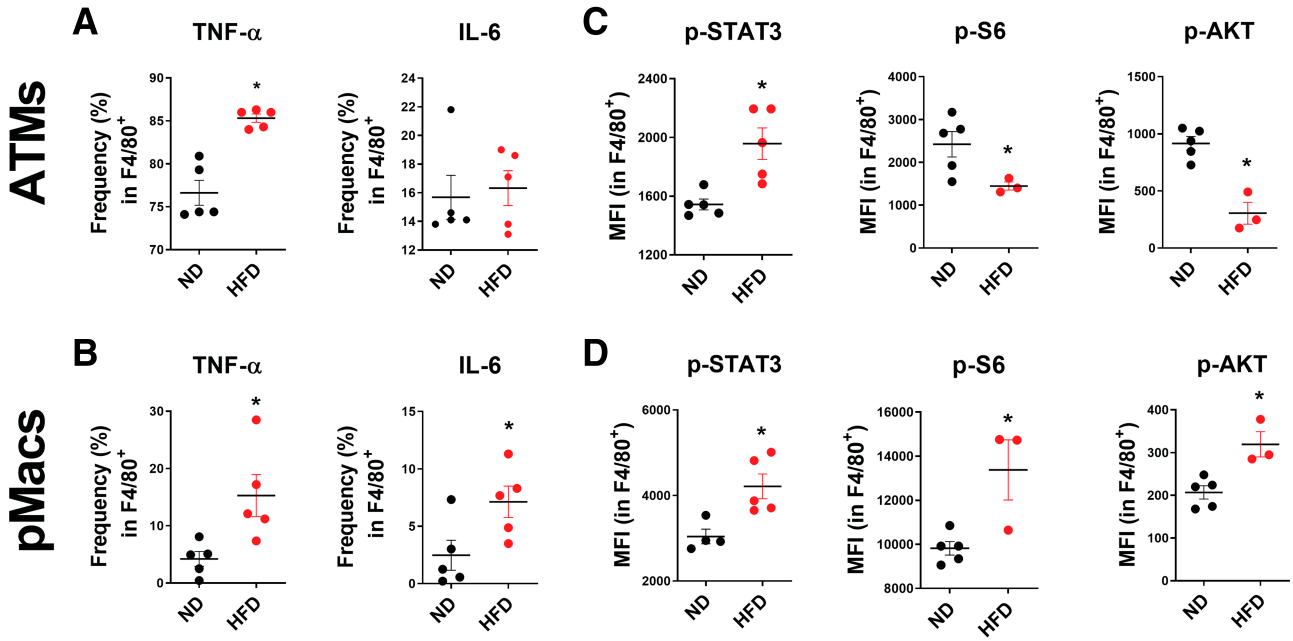

Figure 5—ATMs and pMacs have distinct phenotypes during obesity. *A*: Frequency of TNF-α– and IL-6–positive macrophages from the AT of mice fed a chow ND or an HFD. *B*: Frequency of TNF-α– and IL-6–positive macrophages from the peritoneal lavage of mice fed ND or HFD. *C*: Median fluorescence intensity (MFI) of p-STAT3, p-S6, and p-AKT^{Ser473} in macrophages from the AT of mice fed ND or HFD. *D*: Median fluorescence intensity of p-STAT3, p-S6, and p-AKT^{Ser473} in macrophages from the peritoneal lavage of mice fed ND or HFD. Data are means ± SEM. $n = 5$ per group. *A–D*: Unpaired two-tailed Student *t* test. *$P < 0.05$. Data are representative of three independent experiments. NS, not significant.

that leptin acts as a metabolic and systemic nutritional checkpoint for macrophage response.

Several studies in the literature analyzed the acute effects of leptin on the inflammatory response. Pini et al. (2008) (46) showed that acute leptin injection exacerbated the inflammatory cell infiltrate in *ob/ob* mice using a zymosan-induced model of peritonitis. Conversely, other reports identified acute leptin injection as an important mediator of neutrophil migration and pMacs activation (21,47). Moreover, in another study, Bernotiene et al. (2004) (48) showed that in *ob/ob* and *db/db* mice, loss of leptin or leptin signaling delayed the resolution phase of acute inflammation. They also suggest that the chronic leptin deficiency impairs the control of a proper immune response. This is also evidenced by another work where leptin-deficient mice had increased graft survival due to reduced inflammatory allogeneic response (49). The effect of chronic hyperleptinemia in macrophage activation in obesity is only evident as the mice gain weight and develop metabolic syndrome and endotoxemia (50). Thus, with our in vitro model we were able to characterize the role of leptin-induced macrophage response in an inflammatory environment, such as those induced by obesity (low-grade systemic inflammation). On Mme, macrophages become dysregulated and the loss of leptin signaling nourished the dysfunctional response. Thus, loss of leptin signaling in myeloid cells can improve systemic glucose levels, but during in vitro metabolic activation, similar to what we observed in ATMs in obesity, macrophages become dysregulated and apparently react to the metabolic alterations in the environment in a leptin-independent way.

Circulating LPS leads to activation of tissue-resident immune cells (51). Moreover, the development of obesity and obesity-enhanced gut permeability and the subsequent circulating LPS alter the macrophage population in the AT, leading to increased cell infiltration and imbalance in the pro- and anti-inflammatory phenotypes (M1- and M2-like macrophages) (12,51). AT inflammation and immune dysregulation observed in obese mice result in insulin resistance (3,12,52,53). The majority of previous studies on leptin focused on the systemic effects of this adipokine in metabolism and immunity (*ob/ob* and *db/db* mice) (3,12,52,54–58). These mice display several systemic alterations that can modulate the immune response, and the effects of leptin in these contexts may be indirect, as both of these mouse models (*ob/ob* and *db/db*) are hyperphagic and obese and can develop diabetes, hyperlipidemia, and metabolic endotoxemia (59). Previous reports have shown that LPS induces an increase in circulating levels of leptin, as well as upregulates leptin expression in the AT (60–62). These changes in leptin production are

associated with elevated cytokine levels (TNF, IL-1) and anorexia (62). Obesity is also a major cause of elevated circulating LPS (50,60). As we have shown here, hyperleptinemia profoundly alters LPS-activated macrophage metabolism and response. Moreover, LPS injection in leptin-deficient mice (*ob/ob*) leads to high lethality rates, which can be reversed by leptin treatment (61). This study also shows that leptin deficiency reduces the production of anti-inflammatory cytokines, highlighting the extensive roles of leptin as a pleiotropic adipokine in the immune response (61). When primed to a repair phenotype (IL-4), leptin improves macrophage wound healing capacity that is accompanied by increases in metabolic rates, whereas, when primed with LPS, leptin exacerbates the proinflammatory cytokine production in a glycolysis-dependent way. Leptin can also be produced and released by immune cells, such as regulatory T cells, and plays a negative autocrine role to inhibit the expansion of regulatory T cells (63). In this context, leptin production by the AT and immune cells orchestrates systemic immune response and metabolic changes. The duality of the leptin role in immune activation is deeply rooted in the environmental signals and different cell types that respond via ObR, as observed in the adaptability of ATMs during obesity and the promotion of inflammation by pMacs. Leptin signals in the hypothalamus through activation of the JAK/STAT3 pathway. The majority of the effects of leptin on energy expenditure and glucose homeostasis are described in the context of proopiomelanocortin neuron activation via STAT3, which are anorexigenic neurons that control feeding behaviors (64). In immune cells, there is evidence that for the functional adaptation mediated by leptin treatment, the PI3K/mTOR pathway plays a major role (21). Conversely, we show that lack of STAT3 signaling does not affect leptin-mediated booster in macrophage activation in the same way we observe by inhibiting mTOR activity. Unlike hypothalamic neurons, immune cells are more susceptible to sudden changes in nutrient availability, inflammatory markers (endotoxemia, chemokines, cytokines), and direct interaction with other cell types (12,60). Therefore, it is possible that leptin activates distinct intracellular pathways in different cell types depending on the immunometabolic signal and the appropriate types of response that it demands. Additionally, since the expression of ObR can be modulated by such environmental cues, researchers face an extra challenge, to pin down the beneficial and detrimental roles of leptin.

The obesogenic environment influences ATM inflammatory state (12,65). Hyperleptinemia can be observed in mice 4 weeks after starting chronic HFD feeding. Boutens et al. (66) showed that the AT environment is responsible for ATM metabolic rewiring, specifically, the induction of glycolysis that contributes to ATM proinflammatory trait in obesity. They showed that this process does not depend on leptin alone (66). Here, we show that this appears to occur through a mechanism that involves reduced leptin signaling due to reduced ObR expression in ATMs, as ObR-deficient ATMs from obese mice have the same proinflammatory characteristics as WT ATMs. We suggest that the mechanism underlying systemic inflammation in obesity is not restricted to increased AT inflammation but, rather, involves other tissue-resident cells where ObR expression and signaling are elevated, such as in macrophages residing in the peritoneal cavity.

Leptin potentiated the activation of macrophages by LPS and IL-4. When primed for a specific profile, leptin acts as a checkpoint enhancing immunometabolic features that determine macrophage phenotype. We found that mTOR activation by leptin is necessary for the hyperinflammatory state of activated macrophages. Also, Rictor$^{-/-}$ macrophages presented the same response as ObR$^{-/-}$ cells, indicating that downstream activation of mTORC2 by leptin signaling is sufficient to modulate the inflammation in macrophages. The importance of mTORC2/AKT activation by leptin in bacterial cleansing was also recently shown (67). Genetic deletion of ObR in macrophages reduces proinflammatory cytokine expression, allows for AKT^{Ser473} dephosphorylation, and reduces lysosomal function (67). In a systemic inflammatory condition, such as obesity, impairments in the leptin/mTOR pathway lead to overall improved glucose homeostasis.

Leptin is an abundant hormone present in homeostatic conditions favoring resident and repair phenotypes in macrophages. Under pathological stimuli, aberrant concentrations of leptin in an inflammatory environment favor the proinflammatory phenotype and response of macrophages, which can be directly reflected in the outcome of disease severity and life expectancy. The results of this study raise the possibility that targeting leptin downstream pathways has a great potential for the development of novel therapeutic approaches to treat obesity-induced inflammation and type 2 diabetes. Personalized therapeutic approaches that take into consideration the individual needs of each patient are growing in clinical practices. Due to the different aspects of leptin in the modulation of immune response, targeted therapies for conditions that lead to systemic metabolic disruption (cachexia, anorexia, obesity) should be considered. The use of full knockout models (*ob/ob* and *db/db*) did not allow researchers to fully understand the contribution of leptin signaling in macrophages and other immune and even nonimmune cell types. For example, in *ob/ob* mice, reconstitution of leptin improves metabolic parameters simply because the mice regain their feeding control (behavior) (58). The use of cell-specific knockdown models makes it possible to investigate the effects of leptin on macrophages, reducing the influence of leptin action on other cell types, such as leptin-central actions on energy expenditure, and nutrient availability through fast/feeding. Here, we have shown that selective knockout of leptin receptor in myeloid cells ameliorates the deleterious effects of obesity. Because macrophage activation contributes to systemic low-grade inflammation, limiting leptin signaling in macrophages via selective delivery systems might help reduce inflammation

and restore glucose homeostasis without interfering in other cell types.

Acknowledgments. The authors thank the Metabolomics Core at the Max Planck Institute of Epigenetics and Immunobiology for advice and support of this project.

Funding. This work was supported by the São Paulo research foundation Fundação de Amparo à Pesquisa do Estado de São Paulo (FAPESP) (2013/07607-8, 2015/15262-8, 2016/23328-0, 2019/25973-8, 2019/19435-3, 2018/19338-5, 2019/06372-3, and 2020/16030-0). The authors are also thankful for the support of Max-Planck Society, the Brazilian National Council for Scientific and Technological Development (CNPq), and Coordenação de Aperfeiçoamento de Pessoal de Nível Superior (CAPES), Finance Code 001.

Duality of Interest. No potential conflicts of interest relevant to this article were reported.

Authors Contributions. L.d.B.M. designed, performed, and analyzed experiments, designed figures, and wrote the manuscript. J.S.P., C.F.d.A., F.C.-d.-S., A.C., N.v.T.B., G.G.D., B.C., J.A.d.S.P., J.C., L.M.d.R., G.C., G.R., J.v.V.-d.S., D.A., and S.M.G.D. designed and performed experiments. J.B. designed experiments and analyzed data. S.R.C., J.D., E.J.P., and N.O.S.C. designed experiments and provided reagents. P.M.M.-V. supervised the study, designed experiments, and wrote and edited manuscript. P.M.M.-V. is the guarantor of this work and, as such, had full access to all the data in the study and takes responsibility for the integrity of the data and the accuracy of the data analysis.

References

1. Matarese G, Moschos S, Mantzoros CS. Leptin in immunology. J Immunol 2005;174:3137–3142
2. Moraes-Vieira PMM, Bassi ÊJ, Araujo RC, Câmara NOS. Leptin as a link between the immune system and kidney-related diseases: leading actor or just a coadjuvant? Obes Rev 2012;13:733–743
3. La Cava A, Matarese G. The weight of leptin in immunity. Nat Rev Immunol 2004;4:371–379
4. Maya-Monteiro CM, Bozza PT. Leptin and mTOR: partners in metabolism and inflammation. Cell Cycle 2008;7:1713–1717
5. Monteiro L, Pereira JADS, Palhinha L, Moraes-Vieira PMM. Leptin in the regulation of the immunometabolism of adipose tissue-macrophages. J Leukoc Biol 2019;106:703–716 cited 2022 Feb 10
6. Matarese G, Procaccini C, De Rosa V. The intricate interface between immune and metabolic regulation: a role for leptin in the pathogenesis of multiple sclerosis? J Leukoc Biol 2008;84:893–899
7. Cao H. Adipocytokines in obesity and metabolic disease. J Endocrinol 2014;220:T47–T59
8. Lumeng CN, Bodzin JL, Saltiel AR. Obesity induces a phenotypic switch in adipose tissue macrophage polarization. J Clin Invest 2007;117:175–184
9. McNelis JC, Olefsky JM. Macrophages, immunity, and metabolic disease. Immunity 2014;41:36–48
10. Peraldi P, Hotamisligil GS, Buurman WA, White MF, Spiegelman BM. Tumor necrosis factor (TNF)-alpha inhibits insulin signaling through stimulation of the p55 TNF receptor and activation of sphingomyelinase. J Biol Chem 1996;271:13018–13022
11. Andrade-Oliveira V, Câmara NO, Moraes-Vieira PM. Adipokines as drug targets in diabetes and underlying disturbances. J Diabetes Res 2015;2015:681612
12. Castoldi A, Naffah de Souza C, Câmara NO, Moraes-Vieira PM. The macrophage switch in obesity development. Front Immunol 2016;6:637
13. Lee SM, Choi HJ, Oh CH, Oh JW, Han JS. Leptin increases TNF-α expression and production through phospholipase D1 in Raw 264.7 cells. PLoS One 2014;9:e102373
14. Biswas SK, Mantovani A. Orchestration of metabolism by macrophages. Cell Metab 2012;15:432–437
15. Pearce EL, Pearce EJ. Metabolic pathways in immune cell activation and quiescence. Immunity 2013;38:633–643
16. O'Neill LA, Kishton RJ, Rathmell J. A guide to immunometabolism for immunologists. Nat Rev Immunol 2016;16:553–565
17. Galván-Peña S, O'Neill LAJ. Metabolic reprograming in macrophage polarization. Front Immunol 2014;5:420
18. de Souza Breda CN, Davanzo GG, Basso PJ, Saraiva Câmara NO, Moraes-Vieira PMM. Mitochondria as central hub of the immune system. Redox Biol 2019;26:101255
19. Ieronymaki E, Theodorakis EM, Lyroni K, et al. Insulin resistance in macrophages alters their metabolism and promotes an M2-like phenotype. J Immunol 2019;202:1786–1797
20. Van den Bossche J, O'Neill LA, Menon D. Macrophage immunometabolism: where are we (going)? Trends Immunol 2017;38:395–406
21. Maya-Monteiro CM, Almeida PE, D'Avila H, et al. Leptin induces macrophage lipid body formation by a phosphatidylinositol 3-kinase- and mammalian target of rapamycin-dependent mechanism. J Biol Chem 2008;283:2203–2210
22. Castoldi A, Monteiro LB, van Teijlingen Bakker N, et al. Triacylglycerol synthesis enhances macrophage inflammatory function. Nat Commun 2020;11:4107
23. Moraes-Vieira PM, Castoldi A, Aryal P, Wellenstein K, Peroni OD, Kahn BB. Antigen presentation and T-cell activation are critical for RBP4-induced insulin resistance. Diabetes 2016;65:1317–1327
24. de Brito Monteiro L, Davanzo GG, de Aguiar CF, et al. M-CSF- and L929-derived macrophages present distinct metabolic profiles with similar inflammatory outcomes. Immunobiology 2020;225:151935
25. Monteiro LB, Davanzo GG, de Aguiar CF, Moraes-Vieira PMM. Using flow cytometry for mitochondrial assays. MethodsX 2020;7:100938
26. Buescher JM, Antoniewicz MR, Boros LG, et al. A roadmap for interpreting (13)C metabolite labeling patterns from cells. Curr Opin Biotechnol 2015;189–201
27. Antoniewicz MR, Kelleher JK, Stephanopoulos G. Accurate assessment of amino acid mass isotopomer distributions for metabolic flux analysis. Anal Chem 2007;79:7554–7559
28. Nunes JPS, Dias AAM. ImageJ macros for the user-friendly analysis of soft-agar and wound-healing assays. Biotechniques 2017;62:175–179
29. Buck MD, Sowell RT, Kaech SM, Pearce EL. Metabolic instruction of immunity. Cell 2017;169:570–586
30. Buck MD, O'Sullivan D, Klein Geltink RI, et al. Mitochondrial dynamics controls T cell fate through metabolic programming. Cell 2016;166:63–76
31. Aguer C, Gambarotta D, Mailloux RJ, et al. Galactose enhances oxidative metabolism and reveals mitochondrial dysfunction in human primary muscle cells [published correction appears in PLoS One 2012;7. PLoS One 2011;6:e28536
32. O'Neill LAJ, Artyomov MN. Itaconate: the poster child of metabolic reprogramming in macrophage function. 2019;19:273–281
33. Laplante M, Sabatini DM. mTOR signaling in growth control and disease. 2012;149:274–293
34. Li J, Kim SG, Blenis J. Rapamycin: one drug, many effects. Cell Metab 2014;19:373–379
35. Phung TL, Ziv K, Dabydeen D, et al. Pathological angiogenesis is induced by sustained Akt signaling and inhibited by rapamycin. Cancer Cell 2006;10:159–170
36. Sarbassov DD, Ali SM, Sengupta S, et al. Prolonged rapamycin treatment inhibits mTORC2 assembly and Akt/PKB. Mol Cell 2006;22:159–168
37. Powell JD, Pollizzi KN, Heikamp EB, Horton MR. Regulation of immune responses by mTOR. Annu Rev Immunol 2012;30:39–68
38. Kratz M, Coats BR, Hisert KB, et al. Metabolic dysfunction drives a mechanistically distinct proinflammatory phenotype in adipose tissue macrophages. Cell Metab 2014;20:614–625

39. Huang SC, Smith AM, Everts B, et al. Metabolic reprogramming mediated by the mTORC2-IRF4 signaling axis is essential for macrophage alternative activation. Immunity 2016;45:817–830
40. Moraes-Vieira PM, Yore MM, Dwyer PM, Syed I, Aryal P, Kahn BB. RBP4 activates antigen-presenting cells, leading to adipose tissue inflammation and systemic insulin resistance. Cell Metab 2014;19:512–526
41. Wang CY, Liao JK. A mouse model of diet-induced obesity and insulin resistance. Methods Mol Biol 2012;821:421–433
42. León-Pedroza JI, González-Tapia LA, del Olmo-Gil E, Castellanos-Rodríguez D, Escobedo G, González-Chávez A. [Low-grade systemic inflammation and the development of metabolic diseases: from the molecular evidence to the clinical practice]. Cir Cir 2015;83:543–551 [English edition]
43. Iikuni N, Lam QL, Lu L, Matarese G, La Cava A. Leptin and inflammation. Curr Immunol Rev 2008;4:70–79
44. Ouchi N, Parker JL, Lugus JJ, Walsh K. Adipokines in inflammation and metabolic disease. Nat Rev Immunol 2011;11:85–97
45. Zhou Y, Yu X, Chen H, et al. Leptin deficiency shifts mast cells toward anti-inflammatory actions and protects mice from obesity and diabetes by polarizing M2 macrophages. Cell Metab 2015;22:1045–1058
46. Pini M, Gove ME, Sennello JA, van Baal JWPM, Chan L, Fantuzzi G. Role and regulation of adipokines during zymosan-induced peritoneal inflammation in mice. Endocrinology 2008;149:4080–4085
47. Souza-Almeida G, D'Avila H, Almeida PE, et al. Leptin mediates *in vivo* neutrophil migration: involvement of tumor necrosis factor-alpha and CXCL1. Front Immunol 2018;9:111
48. Bernotiene E, Palmer G, Talabot-Ayer D, Szalay-Quinodoz I, Aubert ML, Gabay C. Delayed resolution of acute inflammation during zymosan-induced arthritis in leptin-deficient mice. Arthritis Res Ther 2004;6:R256–R263
49. Moraes-Vieira PM, Bassi EJ, Larocca RA, et al. Leptin deficiency modulates allograft survival by favoring a Th2 and a regulatory immune profile. [corrected]. Am J Transplant 2013;13:36–44 [corrected]
50. Boutagy NE, McMillan RP, Frisard MI, Hulver MW. Metabolic endotoxemia with obesity: is it real and is it relevant? Biochimie 2016;124:11–20
51. Mohammad S, Thiemermann C. Role of metabolic endotoxemia in systemic inflammation and potential interventions. Front Immunol 2021;11:594150
52. Moraes-Vieira PM, Larocca RA, Bassi EJ, et al. Leptin deficiency impairs maturation of dendritic cells and enhances induction of regulatory T and Th17 cells. Eur J Immunol 2014;44:794–806
53. Matarese G, Procaccini C, De Rosa V, Horvath TL, La Cava A. Regulatory T cells in obesity: the leptin connection. Trends Mol Med 2010;16:247–256
54. Zhou Y, Yu X, Chen H, et al. Leptin deficiency shifts mast cells toward anti-inflammatory actions and protects mice from obesity and diabetes by polarizing M2 macrophages. Cell Metab 2015;22:1045–1058
55. Palhinha L, Liechocki S, Hottz ED, et al. Leptin induces proadipogenic and proinflammatory signaling in adipocytes. Front Endocrinol (Lausanne) 2019;10:841
56. Reis BS, Lee K, Fanok MH, et al. Leptin receptor signaling in T cells is required for Th17 differentiation. J Immunol 2015;194:5253–5260
57. Amar S, Zhou Q, Shaik-Dasthagirisaheb Y, Leeman S. Diet-induced obesity in mice causes changes in immune responses and bone loss manifested by bacterial challenge. Proc Natl Acad Sci U S A 2007;104:20466–20471
58. Harris RBS, Zhou J, Redmann SM Jr, et al. A leptin dose-response study in obese (ob/ob) and lean (+/?) mice. Endocrinology 1998;139:8–19
59. Suriano F, Vieira-Silva S, Falony G, et al. Novel insights into the genetically obese (ob/ob) and diabetic (db/db) mice: two sides of the same coin. Microbiome 2021;9:147
60. Cani PD, Amar J, Iglesias MA, et al. Metabolic endotoxemia initiates obesity and insulin resistance. Diabetes 2007;56:1761–1772
61. Faggioni R, Fantuzzi G, Gabay C, et al. Leptin deficiency enhances sensitivity to endotoxin-induced lethality. Am J Physiol 1999;276:R136–R142
62. Grunfeld C, Zhao C, Fuller J, et al. Endotoxin and cytokines induce expression of leptin, the ob gene product, in hamsters. J Clin Invest 1996;97:2152–2157
63. De Rosa V, Procaccini C, Calì G, et al. A key role of leptin in the control of regulatory T cell proliferation. Immunity 2007;26:241–255
64. Buettner C, Pocai A, Muse ED, Etgen AM, Myers MG Jr, Rossetti L. Critical role of STAT3 in leptin's metabolic actions. Cell Metab 2006;4:49–60
65. Catrysse L, van Loo G. Adipose tissue macrophages and their polarization in health and obesity. Cell Immunol 2018;330:114–119
66. Boutens L, Hooiveld GJ, Dhingra S, Cramer RA, Netea MG, Stienstra R. Unique metabolic activation of adipose tissue macrophages in obesity promotes inflammatory responses. Diabetologia 2018;61:942–953
67. Fischer J, Gutièrrez S, Ganesan R, et al. Leptin signaling impairs macrophage defenses against *Salmonella* typhimurium. Proc Natl Acad Sci U S A 2019;116:16551–16560